

This is an Open Access document downloaded from ORCA, Cardiff University's institutional repository: <https://orca.cardiff.ac.uk/id/eprint/165721/>

This is the author's version of a work that was submitted to / accepted for publication.

Citation for final published version:

Yin, Ruonan, Xue, Bo, Brousseau, Emmanuel , Geng, Yanquan and Yan, Yongda 2024. Characterizing the electric field- and rate-dependent hysteresis of piezoelectric ceramics shear motion with the Bouc-Wen model. *Sensors and Actuators A: Physical* 367 , 115044. 10.1016/j.sna.2024.115044

Publishers page: <https://doi.org/10.1016/j.sna.2024.115044>

Please note:

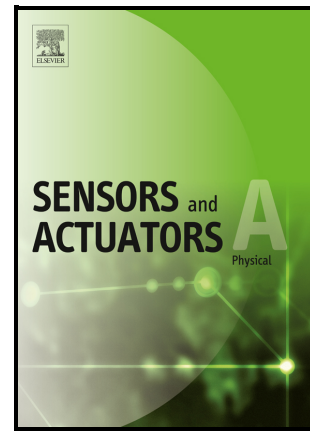
Changes made as a result of publishing processes such as copy-editing, formatting and page numbers may not be reflected in this version. For the definitive version of this publication, please refer to the published source. You are advised to consult the publisher's version if you wish to cite this paper.

This version is being made available in accordance with publisher policies. See <http://orca.cf.ac.uk/policies.html> for usage policies. Copyright and moral rights for publications made available in ORCA are retained by the copyright holders.



Characterizing the electric field- and rate-dependent hysteresis of piezoelectric ceramics shear motion with the Bouc-Wen model

Ruonan Yin, Bo Xue, Emmanuel Brousseau, Yanquan Geng, Yongda Yan



PII: S0924-4247(24)00037-2

DOI: <https://doi.org/10.1016/j.sna.2024.115044>

Reference: SNA115044

To appear in: *Sensors and Actuators: A. Physical*

Received date: 19 September 2023

Revised date: 19 December 2023

Accepted date: 15 January 2024

Please cite this article as: Ruonan Yin, Bo Xue, Emmanuel Brousseau, Yanquan Geng and Yongda Yan, Characterizing the electric field- and rate-dependent hysteresis of piezoelectric ceramics shear motion with the Bouc-Wen model, *Sensors and Actuators: A. Physical*, (2024)  
doi:<https://doi.org/10.1016/j.sna.2024.115044>

This is a PDF file of an article that has undergone enhancements after acceptance, such as the addition of a cover page and metadata, and formatting for readability, but it is not yet the definitive version of record. This version will undergo additional copyediting, typesetting and review before it is published in its final form, but we are providing this version to give early visibility of the article. Please note that, during the production process, errors may be discovered which could affect the content, and all legal disclaimers that apply to the journal pertain.

# Characterizing the electric field- and rate-dependent hysteresis of piezoelectric ceramics shear motion with the Bouc-Wen model

Ruonan Yin<sup>a</sup>, Bo Xue<sup>a\*</sup>, Emmanuel Brousseau<sup>b</sup>, Yanquan Geng<sup>c</sup>, Yongda Yan<sup>c</sup>

<sup>a</sup> College of Mechanical and Electrical Engineering, Northeast Forestry University, Harbin, China

<sup>b</sup> Cardiff School of Engineering, Cardiff University, Cardiff, United Kingdom

<sup>c</sup> Center for Precision Engineering, Harbin Institute of Technology, Harbin, China

\*Corresponding author: xb\_356@163.com

## Abstract

Piezoelectric technology is widely used in the field of precision drives. However, when piezoelectric actuators are employed at high voltages and high frequencies, their hysteresis can greatly affect the accuracy of such systems. The Bouc-Wen model has typically been used by researchers to characterise the hysteresis of piezoelectric materials. Besides, to extract the parameters of this model from experimental data, particle swarm optimization (PSO) is often employed. However, the majority of such studies only considers hysteresis as a function of the electric field strength and not as a function of actuation frequency. In addition, most of such existing reports have focused on longitudinal type piezo actuators. In this context, the research presented here complements this body of knowledge by demonstrating the application of the PSO algorithm for determining the parameters of the Bouc-Wen model when hysteresis depends not only on the electric field but also on the rate of the driving signal and when applied on a shear-type piezoelectric actuator. The obtained experimental data showed that that with the increase of electric field strength, both the piezoelectric coefficient and hysteresis value increased significantly, and that with the increase of frequency, the piezoelectric coefficient decreased, while the hysteresis value changed slightly. The variations of the Bouc-Wen model parameters with the electric field and frequency were identified and then used to predict the shear motion trajectory of the piezoelectric stack. It was found that in the identified range of electric field and frequency, the predicted error rate of the hysteresis loop amplitude was less than 16.5%

with a minimum value of 0.1%, and the error rate of the hysteresis loop width was less than 14.5% with a minimum value of 2.7%. Based on the identified electric field- and rate-dependent Bouc-Wen model, a novel finite element (FE) model was also proposed to analyse the effect of electrical and mechanical coupling on the piezoelectric movement.

**Keywords:** Shear motion of piezoelectric ceramics, electric field- and rate-dependent hysteresis, Bouc-Wen model, PSO, finite element analysis

## 1. Introduction

Based on the high speed, high resolution and high accuracy [1] of piezoelectric ceramic materials, piezoelectric drive technology has been widely employed in fields such as precision positioning [2], microfluidic actuation [3], biomedical technology [4] and aerospace [5]. However, hysteresis is inherent in such systems and results in nonlinearity with multivalued mapping between the electric field and the strain. With the electric field strength increasing, the nonlinearity of the direct piezoelectric effect, and hence of the strain, becomes more pronounced [6, 7]. Furthermore, when the frequency of the electric field changes, the relationship between strain and electric field also exhibits a rate-dependent behaviour [8, 9]. The positioning error caused by the hysteresis of piezoelectric ceramics can reach 15% of the displacement range, which seriously affects the precision of piezoelectric actuators [10]. Therefore, it is very important to characterize the nonlinear properties of piezoelectric ceramics.

A number of mathematical models have been established to characterize the hysteresis of piezoelectric materials. These models can be used to compensate for the nonlinear error in a closed-loop feedback system. These models can be mainly divided into two types, namely operator-based models and differential-based models [11]. The Prandtl-Ishlinskii (PI) hysteresis model is frequently employed among operator-based models. For example, Ru et al. modified the PI model by using a least mean square method to identify the weight of the main hysteresis loop and applied this approach to the inverse feedforward controller of a piezoelectric actuator [12]. Gu et al. used an

improved PI model to characterize the inverse hysteresis effect of piezoelectric actuators. More specifically, these authors implemented an adaptive particle swarm optimization (PSO) algorithm to identify the model parameters and implemented a real-time feedforward controller that could reduce the tracking error caused by hysteresis by about one order of magnitude [13]. Al Janaideh et al. proposed two different temperature-dependent nonlinear hysteresis models based on an electromechanical model and a PI model to consider the effect of temperature on hysteresis [14]. Among the differential-based models, the Bouc-Wen formalism is widely used to characterize the nonlinear hysteresis behaviour of piezoelectric ceramics. Most of such research efforts follow a “black box” approach for which a set of experimental input and output data is collected first to subsequently adjust the parameters of the Bouc-Wen formula so that the output of the model eventually matches the experimental data. For a specific input, the Bouc-Wen model can provide a good alignment with experiments. However, such a “black box” approach does not explain important physical properties inherent of the behaviour of the system [15]. Zhu and Wang introduced an asymmetric formulation in the Bouc-Wen hysteresis operator to model the asymmetric hysteresis of piezoelectric ceramic actuators and reported an improvement in the prediction accuracy by about 30% [16]. Wang et al. modified the Bouc-Wen model to describe this asymmetry and proposed a parameter identification method based on the modified differential evolution (MDE) algorithm [17]. These authors showed that the MDE approach compared favourably against the classical differential evolution algorithm. Based on the Bouc-Wen model and the inverse multiplicative structure, Rakotondrabe proposed a new method for compensating hysteresis nonlinearity in smart materials, especially for piezoelectric actuators, which is relatively straightforward to implement [18]. Piezoelectric actuators exhibit rate-dependent hysteresis nonlinearities that increase as the frequency of the applied input increases [19]. In this case, rate-dependent hysteresis models are developed to indicate the influence of the changing rate of the input voltage [20]. Rate dependent hysteresis formulations are usually realized by introducing rate dependent function into the model, such as employing dynamic envelope functions into the play operators of PI model [21] and proposing a

dynamic inverse operator by combining rate-dependent dissipation function with the first-order restoring curve [22]. For describing the rate-dependent hysteresis of piezoelectric ceramic actuators under high frequency excitation, Gan and Zhang introduced an input frequency factor into the classical Bouc-Wen model and decreased the prediction error by about 75% [23]. Meanwhile, aiming at the rate-dependent behaviour of the hysteresis phenomenon of piezoelectric actuators, Kang et al. established a fractional-order normalized Bouc-Wen model by adopting a n-order polynomial input function and two fractional operators, resulting in better modelling accuracy and hysteresis compensation as compared to the traditional improved model [24]. Additionally, the Bouc-Wen model has also been used to characterize other hysteresis phenomena. For example, Muthalif et al. used a modified model to analyse the hysteresis of magnetorheological (MR) damper [25]. By calculating the Bouc-Wen model parameters as a function of current and frequency, equations describing MR damper dynamics were obtained.

While many studies have been conducted to characterize the nonlinear behaviour of the longitudinal extension of piezoelectric actuator resulting from hysteresis, there is relatively little research focused on tackling the same issue for the shear-type piezoelectric actuators. Such actuators can supply bending and translational motions [26]. Furthermore, no study comprehensively investigated the electric field and rate dependence of the hysteresis nonlinearity in the shear motion produced by such piezoelectric actuators. In recent years, in the field of nanofabrication, piezoelectric shear stacks have been proposed to act as a spindle to drive the cutting tool and implement the nanomilling process to fabricate nanostructures [27, 28]. However, it is also critical when implementing nanomilling to be able to control the tool trajectory accurately in order to ensure machining quality. To address this need, this paper presents a method for characterising the moving trajectory of shear-type piezoelectric ceramics under high electric field and high frequency excitation based on the Bouc-Wen model. In particular, it is proposed to introduce the electric field and rate dependences into the model.

The structure of the study is as follows: first, the electric field and rate dependence

of the hysteresis behaviour of a shear-type piezoelectric actuator analysed based on obtained experimental displacement data. Second, the Bouc-Wen model is identified using the PSO algorithm and used to describe the hysteresis nonlinearity by fitting the variations of the identified parameters with the electric field and frequency. Then, the prediction accuracy of the proposed method is evaluated against the electric field and rate dependence laws of nonlinear hysteresis in piezoelectric ceramics. Finally, an example of piezoelectric displacement analysis under the electrical and mechanical coupled effect is given by combining the proposed method with finite element analysis.

## 2. Methods

### 2.1 Bouc-Wen model

The Bouc-Wen model is essentially a first-order nonlinear differential equation, which relates the input displacement to the output restoring force in a hysteretic way. The response of the model to the real hysteresis loops can be adapted by an appropriate choice of a set of parameters, which in general can be expressed as follows:

$$\dot{z} = A\dot{u} - \beta|\dot{u}|z|z|^{n-1} - \gamma\dot{u}|z|^n \quad (1)$$

where the parameters  $A$ ,  $\beta$  and  $\gamma$  determine the shape of the hysteresis loop and  $n$  is an integer.  $z$  in the equation is the state variable, integrated by the state space equation of the system, and  $\dot{u}$  is the derivative of the existing input [29, 30].

When the Bouc-Wen model is used to represent the hysteresis characteristics of a piezoelectric actuator, the total number of parameters can be reduced to six through suitable simplification and constraint. By introducing the input bias and asymmetric factors, the modified Bouc-Wen model can effectively describe the hysteresis process. The specific model expression is shown as follows [30, 31]:

$$h(\dot{t}) = \alpha u(\dot{t}) - \beta|u(\dot{t})||h(\dot{t})|^{n-1}h(\dot{t}) - \gamma u(\dot{t})|h(\dot{t})|^n + \Delta\varepsilon \quad (2)$$

$$\Delta\varepsilon = \eta u(\dot{t}) \operatorname{sgn}(u(\dot{t})) \quad (3)$$

$$y_{bw}(\dot{t}) = k_1 u(\dot{t}) + k_2 h(\dot{t}) \quad (4)$$

where  $h(\dot{t})$  is the nonlinear hysteresis term,  $u(\dot{t})$  is the input voltage,  $y_{bw}(\dot{t})$  is

the output displacement,  $\alpha$ ,  $\beta$ ,  $\gamma$ ,  $k_1$ ,  $k_2$ ,  $\eta$  are the parameters determining the shape of the hysteresis loop and which need to be identified,  $n$  determines the hysteresis loop sharpness and  $\Delta\varepsilon$  is the asymmetric hysteresis factor. The Bouc-Wen model can be used to characterize or predict the hysteresis behavior after its parameters are identified by appropriate algorithms.

## 2.2 Particle swarm optimization (PSO) algorithm

Several algorithms can be used to identify the Bouc-Wen model parameters listed in Eq. (2), e.g., least square method [16], difference algorithm [17] and PSO [25, 32]. The PSO approach is more widely used due to its simple concept, ease of implementation and fast convergence [33]. Since the initial version of the PSO algorithm was not very effective [34], an improved PSO algorithm was proposed soon after [35], which introduces inertia weights in the velocity update formula. Larger inertia weights facilitate exploratory search while smaller inertia weights contribute to exploitative search, and hence dynamic inertia weights are essential [36]. Clerc and Kennedy introduced a variant into the PSO algorithm with a shrinkage factor  $\chi$  when analysing the convergence, which was able to increase the convergence speed and prevents the solution from falling into a local extremum [37]. The shrinkage factor is expressed as follows:

$$\chi = \frac{2}{|2 - \xi + \sqrt{\xi^2 - 4\xi}|} \quad (5)$$

$$\xi = c_1 + c_2, \xi > 4 \quad (6)$$

The final improved PSO algorithm speed and position update equation obtained is given by:

$$v_{i,t+1}^d = \chi_i * \omega_i * v_{i,t}^d + c_1 * rand * (p_{i,t}^d - x_{i,t}^d) + c_2 * rand * (p_{g,t}^d - x_{i,t}^d) \quad (7)$$

$$x_{i,t+1}^d = x_{i,t}^d + v_{i,t+1}^d \quad (8)$$

where  $\omega_i$  is the dynamic inertia weight and is expressed as  $\omega_i = \omega_{max} - ((\omega_{max} - \omega_{min})/N) * i$ .  $\omega_{max}$  and  $\omega_{min}$  are obtained through a trial-and-error approach with commonly chosen values being between 0.9 and 0.1, respectively.

### 2.3 Displacement measurement of the shear-type piezoelectric stack

For achieving reliable measurements of the high frequency displacements of piezoelectric actuators, laser interferometry is commonly employed [38, 39]. In this paper, a one-dimensional laser Doppler vibrometer (LDV) (model OFV-303 from Polytec, Germany) was chosen to measure the shear motion displacements of a piezoelectric ceramic shear-type stack (model NAC2902-H2.8 from Noliac, Denmark). This actuator has a maximum stroke of 1.5  $\mu\text{m}$  under the operating voltage of  $\pm 320$  V. Fig. 1 shows the details of the experimental set-up of piezoelectric system. By considering the stiffness degradation of epoxy resin at high frequencies, the piezoelectric shear-type stack is fixed by the mechanical clamping instead of gluing. The bottom end plate of the stack with a thickness of up to 1 mm is mechanically clamped by a screw and two fixtures onto a base. An excitation signal generated by the signal generator (model Wave Station 2012 from Teledyne Lecroy, USA) is amplified by the power amplifier (model 2100HF from Trek, USA) with a fixed gain of 50 V/V, and then applied to the piezoelectric stack. The excitation signals considered in this work are listed in Table 1. The oscilloscope is used to simultaneously collect the excitation signal and the displacement response signal as depicted in Fig. 1. The shear actuator plate in the piezoelectric stack had a thickness of 0.5 mm, and the electric field applied to it can be calculated by dividing the driving voltage by the thickness.

Table 1 Specific parameters of the excitation signal

Driving voltage ( $V_{pp}$ )	50, 62.5, 75, 87.5, 100, 112.5, 125
Driving frequency (Hz)	100, 200, 400, 600, 800, 1000

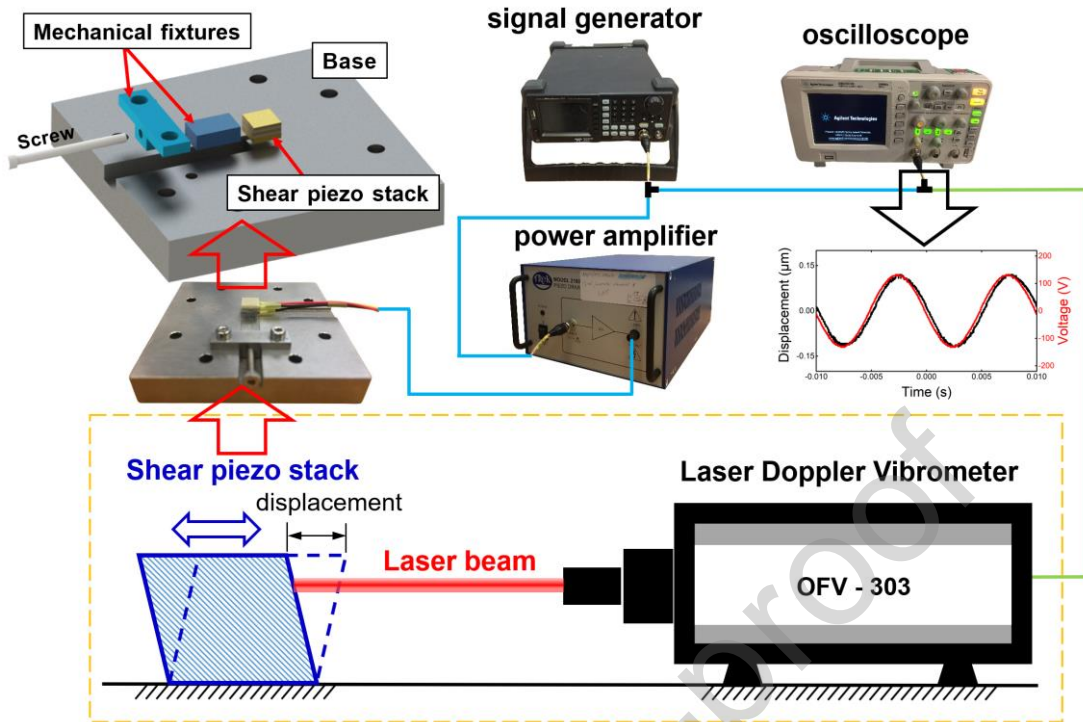


Fig. 1 Schematic diagram for measuring the displacement of the piezoelectric stack.

### 3. Results and Discussion

#### 3.1 Analysis of the hysteresis of the shear-type piezoelectric stack

Fig. 2 (a) and (b) shows an example of the input and output data which were collected under the driving conditions of 75 V and 200 Hz. The collected displacement signal contains the useful information related to the motion of the piezo-based system and the useless information caused by the electronic noise, which are located in different frequency domains. Due to higher bandwidths of the LDV and the oscilloscope, the noise signals are the higher order harmonic components of the displacement signal. It was found that the noise in the original data had a serious impact on the following hysteresis analysis and parameter identification. Hence, the Fast Fourier Transform (FFT) filtering was first employed to eliminate the high frequency noise in the experimental data. To avoid filtering out the useful harmonic components, it is very important to determine the cut-off frequency of the FFT low-pass filter. It was obtained through trial-and-error method that the optimal cut-off frequency of filtering was set to be 5 times higher than the frequency of the voltage signal, i.e. the fundamental frequency, which could effectively remove high frequency noise and have little effect

on the harmonic components related to the nonlinear hysteresis motion in the original data. In Fig. 2(c), three examples of original experimental data under different voltages and frequencies are selected to compare with their filtered data. It can be seen that all three smooth curves coincide well with their original curves, indicating that the noise is eliminated without compromising hysteresis characteristics.

Fig. 3(a)-(f) show the comprehensive set of hysteresis loops obtained under some combinations of voltages and frequencies, as listed in Table 1. It can be seen that for each frequency, the shape of the loop enlarges with the increase in voltage, while for a given voltage, the shape of the loop does not change significantly with the frequency except for a small clockwise rotation as shown in Fig. 3(d)-(f). The theoretical characterization of the hysteresis loop has been the focus of numerous research efforts. Ikhouane et al. [40] studied the effects of the parameters of the normalized Bouc-Wen model on the shape of the hysteresis loop. These authors used the maximum value and the zero-point variation of the loop to describe the hysteresis. When analysing the influences of different parameters of the Bouc-Wen model on the hysteresis, Zhang et al. described the shape of the loop with its width, rotation direction, curvature and amplitude [41]. In this paper, three geometric parameters are adopted, as depicted in Fig. 3(f), namely the maximum amplitude values of displacement ( $A_{Max}$ ), voltage ( $V_{Max}$ ) and the maximum vertical width ( $W_{Max}$ ). These parameters were evaluated and then used to calculate the piezoelectric coefficient ( $d_{15}$ ) and hysteresis value ( $H_{disp}$ ). In particular,  $d_{15}$  is obtained by expressing the slope between the switching points of the hysteresis loop, as follows:

$$d_{15} = \frac{\text{Strain (S)}}{\text{Electric field (E)}} = \frac{A_{Max}}{V_{Max}} \quad (9)$$

while  $H_{disp}$  is defined as the ratio of the opening width of the hysteresis loop to the maximum displacement, according to the following equation:

$$H_{disp} = \frac{W_{Max}}{A_{Max}} \quad (10)$$

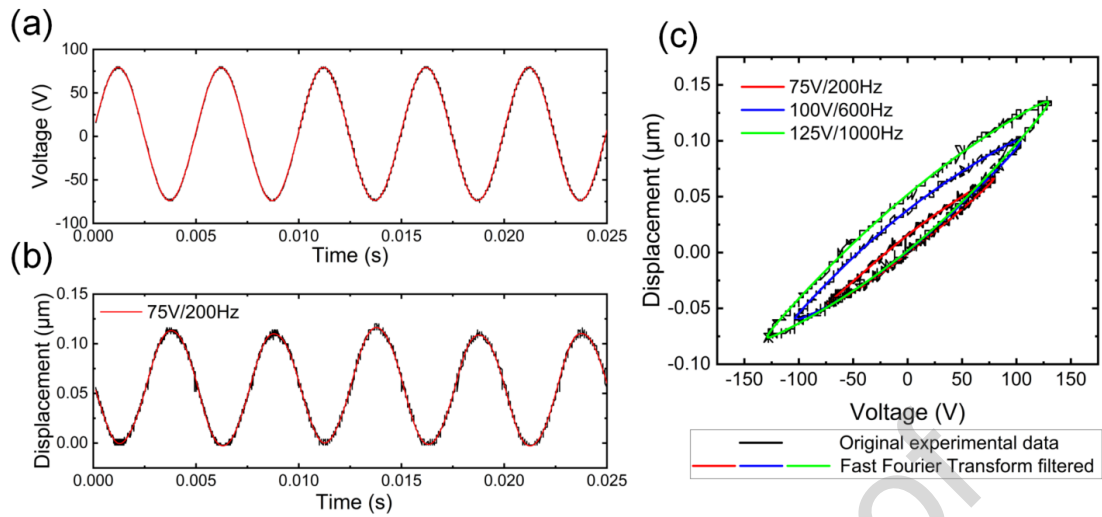


Fig. 2 (a) An example of input excitation voltage and its FFT processing, (b) the corresponding output response displacement and its FFT processing, and (c) the comparison of hysteresis curves of the original experimental data and the data processed by FFT under different voltages and frequencies.

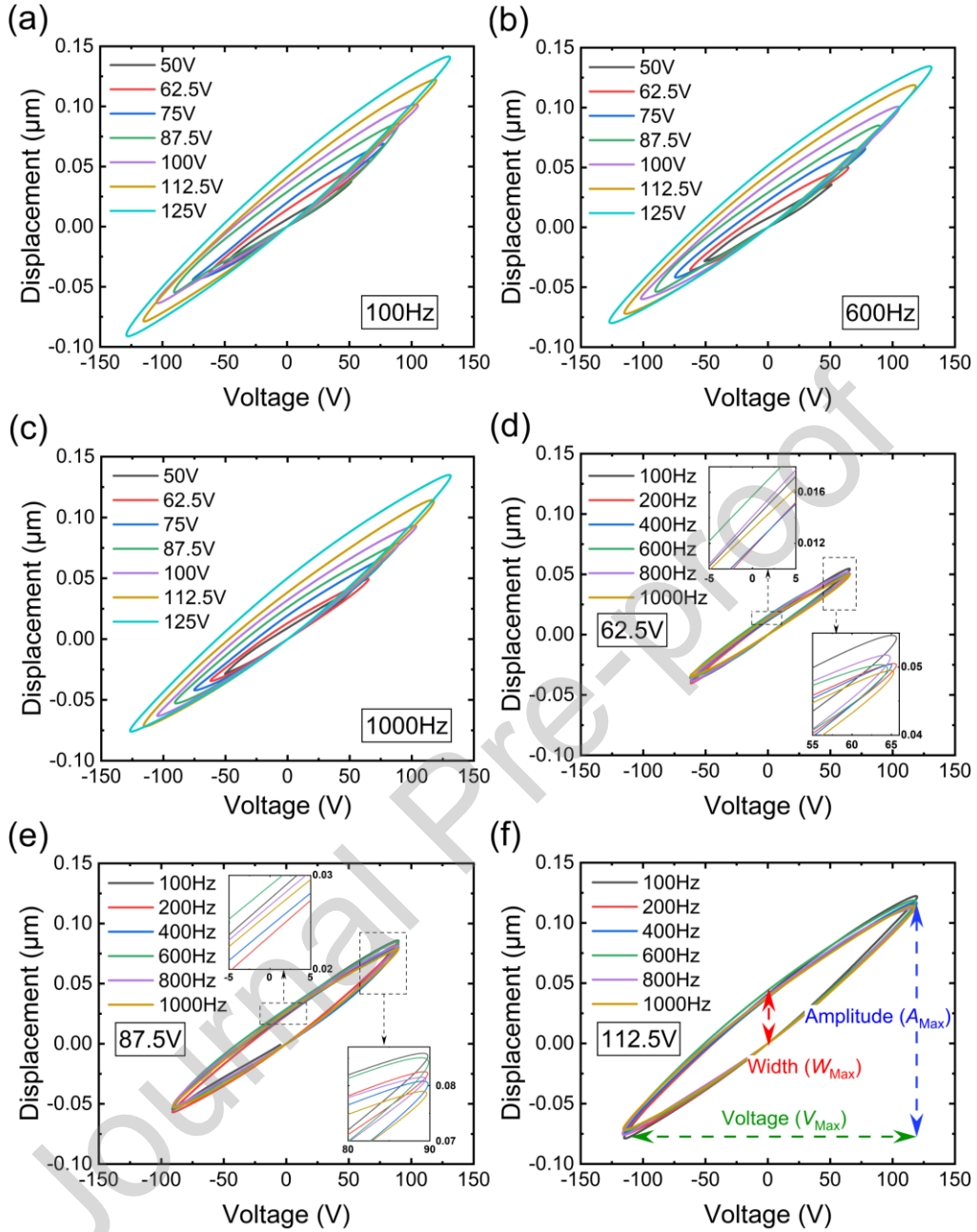


Fig. 3 Hysteresis loops of the shear motion of piezoelectric stack actuated under different frequencies of (a) 100Hz, (b) 600Hz, (c) 1000Hz and voltages of (d) 62.5V, (e) 87.5V, (f) 112.5V.

Fig. 4 show the variations of the maximum amplitudes of displacement ( $A_{Max}$ ) and the maximum vertical width ( $W_{Max}$ ) with different electric fields and frequencies. Fig. 5 and Fig. 6 show the variations of piezoelectric coefficient ( $d_{15}$ ) and hysteresis value ( $H_{disp}$ ) with different electric fields and frequencies. It can be seen from Fig. 5(a)-(c) that  $d_{15}$  increases with the electric field intensity and decreases when the frequency

becomes higher. As shown in Fig. 6(a)-(c),  $H_{disp}$  increases as the electric field strength increases, while it is less affected by the frequency in the chosen range. Thus, it can be said that compared to the frequency, the electric field intensity plays a major role in the displacement of the piezoelectric shear actuator. This is consistent with the results of previous studies [42].

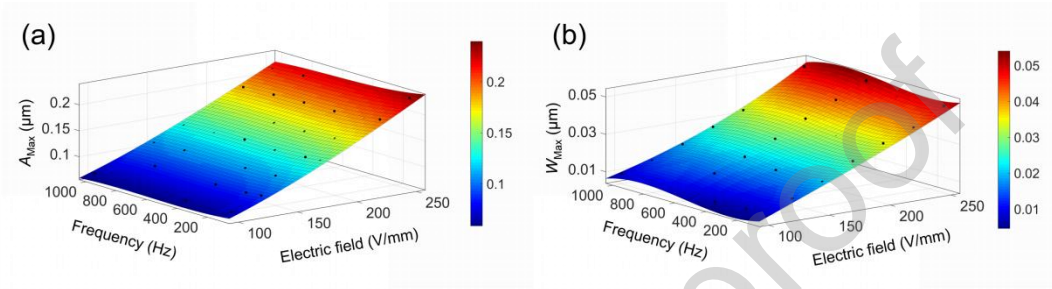


Fig. 4 Variations of loop amplitude (a) and width (b) for different electric fields and frequencies.

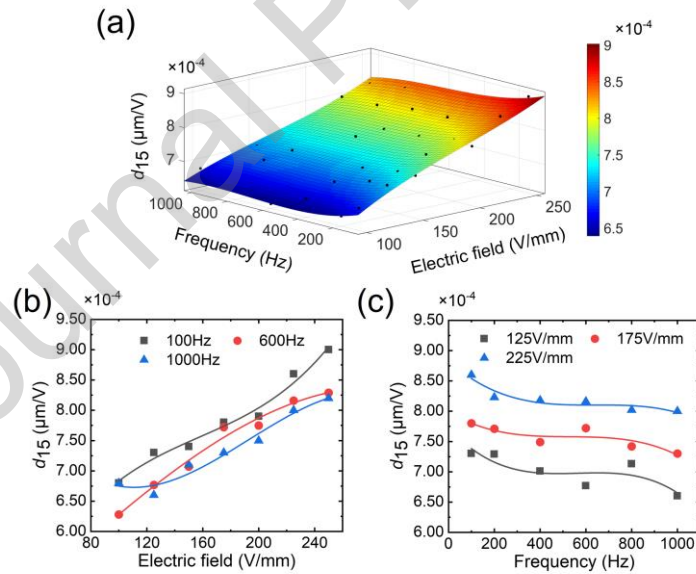


Fig. 5 Variation of the piezoelectric coefficient as a function of electric field and frequency (a), value of the piezoelectric coefficient with electric field at three frequencies (b), value of the piezoelectric coefficient with frequency at three electric fields (c).

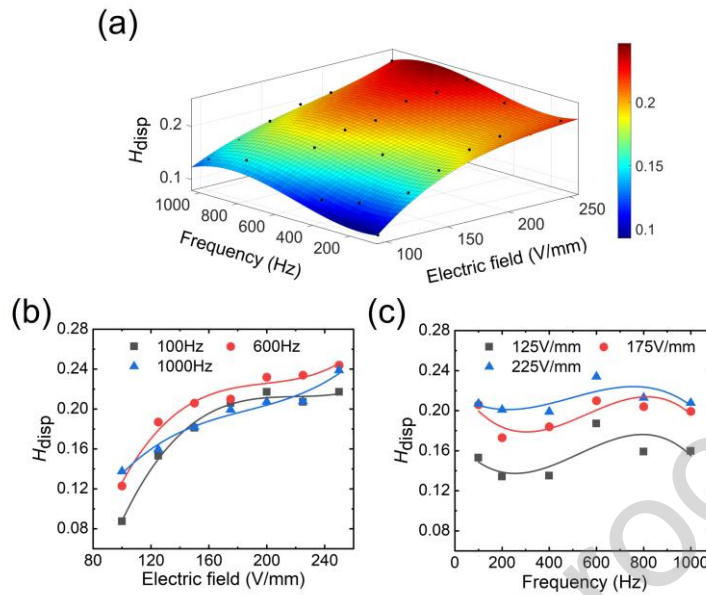


Fig. 6 Variation of the hysteresis value as a function of electric field and frequency (a), hysteresis value against electric field at three frequencies (b), hysteresis value against frequency at three electric fields (c).

The reason why the piezoelectric coefficient and hysteresis values vary with the electric field strength and frequency is due to the motions of the domain walls inside the piezoelectric ceramic. The origin of the hysteretic nonlinear behaviour of piezoelectric ceramics has been characterised in many studies. Li et al. concluded that the nonlinear phenomenon observed in ferroelectric ceramics was mainly caused by the nonlinear motion of the non-180° domain wall [43]. By investigating the contribution of domain wall motion to the response of PZT-based ceramics, Garcia et al. found that the piezoelectric response of piezoelectric ceramics was a result of the superposition of the intrinsic contribution (deformation of crystalline element cells) and extrinsic contribution (movement of domain walls) [44]. Hysteresis is related to the irreversible motion of domain walls. In addition, the mobility of a domain wall is related to the spontaneous strain level of the crystal structure, and the high level of spontaneous strain would make domain wall movement difficult. Mojca et al. found that domain wall motion and lattice strain were the main mechanisms of dielectric and piezoelectric response of ferroelectric ceramics by using in-situ diffraction method [45]. Their analysis of different PZT samples showed that the nonlinear hysteresis in the

macroscopic piezoelectric response of soft PZT was caused by the motion of non 180° domain walls. As discussed above, it can be said that the nonlinearity of the piezoelectric response is mainly caused by the non-180° domain wall motion, and the hysteresis is related to the irreversible motion of domain walls. With the increase of the electric field strength, both the number of non-180° domain walls starting to move, and the corresponding motion intensity increases, and at the same time, the number of irreversible domain wall motion increases, which results in the piezoelectric coefficient and hysteresis value increasing with the increase of electric field intensity. Fig. 5(b) and Fig. 6(b) displays this field-dependent property. Kannan and Kochmann conducted in-situ experiments to investigate the effect of the electric loading rate on ferroelectric domain switching in barium titanate ceramics, and showed that the domain wall motion reduces at higher electric field rates [46]. With the frequency of the applied electric field increasing, the change of domain wall motion cannot keep up with the change in excitation, which in turn leads to fewer motion of walls and hence the decrease of the piezoelectric coefficient. It has also been reported that hysteresis is rate-related and that it increases with the increase of the input rate [47, 48]. Similarly, the main reason is that higher changing rate would cause a smaller number of irreversible domain wall motions. However, this rate dependency is not obvious in Fig. 5(c) and Fig. 6(c). It may be due to the different type of piezoelectric ceramic material employed here and that the electric field level applied was not large enough to reflect this.

The variations of hysteresis loop amplitude and width, the piezoelectric coefficient and the hysteresis value versus electric field strength and frequency were fitted to polynomial surfaces. Correspondingly, bivariate cubic polynomial functions were obtained with the arguments of electric field strength in the range from 100 V/mm to 250 V/mm and electric field frequency in the range from 100 Hz to 1000 Hz, as follows:

$$C(E, f) = C_{00} + C_{10} * E + C_{01} * f + C_{20} * E^2 + C_{11} * E * f + C_{02} * f^2 + C_{30} * E^3 + C_{21} * E^2 * f + C_{12} * E * f^2 + C_{03} * f^3 \quad (11)$$

where  $E$  is the strength of the electric field,  $f$  is the frequency of the electric field and  $C_{xx}$  are the coefficients of the function.

The fitted binary cubic polynomial function coefficients are listed in Table 2, and the corresponding fitting errors are given in Table 3. It can be observed that the sum of squared errors (SSE) is very small, and the coefficients of determination (R-Square) are all around 0.9, indicating a reasonable goodness of fit. Given the determination of the fitted functions, the effectiveness of the prediction of the displacement by the proposed model could be verified, as reported in the following section.

Table 2 Coefficient values of the binary cubic polynomial function related to hysteresis loop amplitude and width, piezoelectric coefficient and hysteresis value.

$C_{xx}$	$A_{Max}(E, f)$	$W_{Max}(E, f)$	$d_{15}(E, f)$	$H_{disp}(E, f)$
$C_{00}$	$1.83 \times 10^{-2}$	$-1.75 \times 10^{-2}$	$4.07 \times 10^{-4}$	$-2.14 \times 10^{-1}$
$C_{10}$	$2.50 \times 10^{-4}$	$3.00 \times 10^{-4}$	$4.26 \times 10^{-6}$	$4.93 \times 10^{-3}$
$C_{01}$	$-3.42 \times 10^{-5}$	$-1.85 \times 10^{-5}$	$-1.82 \times 10^{-7}$	$3.49 \times 10^{-5}$
$C_{20}$	$3.42 \times 10^{-6}$	$-3.26 \times 10^{-7}$	$-1.64 \times 10^{-8}$	$-1.89 \times 10^{-5}$
$C_{11}$	$-8.40 \times 10^{-8}$	$-1.90 \times 10^{-7}$	$-7.38 \times 10^{-10}$	$-1.94 \times 10^{-6}$
$C_{02}$	$7.90 \times 10^{-8}$	$8.28 \times 10^{-8}$	$4.05 \times 10^{-10}$	$4.06 \times 10^{-7}$
$C_{30}$	$-3.88 \times 10^{-9}$	$9.15 \times 10^{-10}$	$2.90 \times 10^{-11}$	$2.50 \times 10^{-8}$
$C_{21}$	$-2.58 \times 10^{-10}$	$5.37 \times 10^{-10}$	$1.70 \times 10^{-12}$	$4.66 \times 10^{-9}$
$C_{12}$	$7.52 \times 10^{-11}$	$-4.50 \times 10^{-12}$	$-1.18 \times 10^{-13}$	$1.75 \times 10^{-10}$
$C_{03}$	$-4.94 \times 10^{-11}$	$-5.16 \times 10^{-11}$	$-1.97 \times 10^{-13}$	$-2.88 \times 10^{-10}$

Table 3 Polynomial fitting errors of the hysteresis parameters.

Error parameter	$A_{Max}$	$W_{Max}$	$d_{15}$	$H_{disp}$
SSE	1.68E-04	9.25E-05	7.24E-09	5.94E-03
R-Square	0.9985	0.9883	0.9581	0.8902

### 3.2 Electric field- and rate-dependent Bouc-Wen model

Based on the measured displacement data of the piezoelectric ceramic shear motion as reported in Section 2.3, the six parameters of the improved Bouc-Wen model,  $\alpha$ ,  $\beta$ ,  $\gamma$ ,  $k_1$ ,  $k_2$  and  $\eta$ , were identified by using the PSO algorithm under different driving voltages and frequencies. The mean square error (MSE) between the experimental data and the identification data was selected as the objective function of

PSO algorithm. MSE reflects the degree of difference between the estimator and the estimand, which is often used as the objective function of the iterative convergence process. The equation of objective function is as follows:

$$F(\alpha, \beta, \gamma, k_1, k_2, \eta) = \frac{1}{L} \sum_{i=1}^L (y - y_{BW})^2 \quad (12)$$

where  $L$  is the number of experimental samples,  $y$  is the experimental data, and  $y_{BW}$  is the identification data calculated by Eqs. (2)-(4). The range of the six parameters to be identified is set to be from -100 to 100, the population size is 200, the maximum number of iterations is set to be 300, and the particle velocity range is from -1 to 1. Fig.7 shows the evaluation of the six parameters of the Bouc-Wen model, and the MSE of the experimental data and the identification data in the iterative process. Fig.8 shows three examples of displacement data calculated by the identified Bouc-Wen model as compared with the experimental data ((a)-(c)) as well as the comparisons between predicted and measured hysteresis loops ((d)-(f)). It can be seen from these plots that a reasonable agreement was obtained under all considered conditions. The MSE value of the identified hysteresis loop, as compared to the experimental hysteresis loop, under each condition was also calculated. It can be observed that for each frequency considered the accuracy of the identification decreases as the voltage increases, and that this effect becomes more prominent with a higher frequency. However, the overall MSE is relatively small, indicating a reasonable model accuracy in the selected voltage and frequency range.

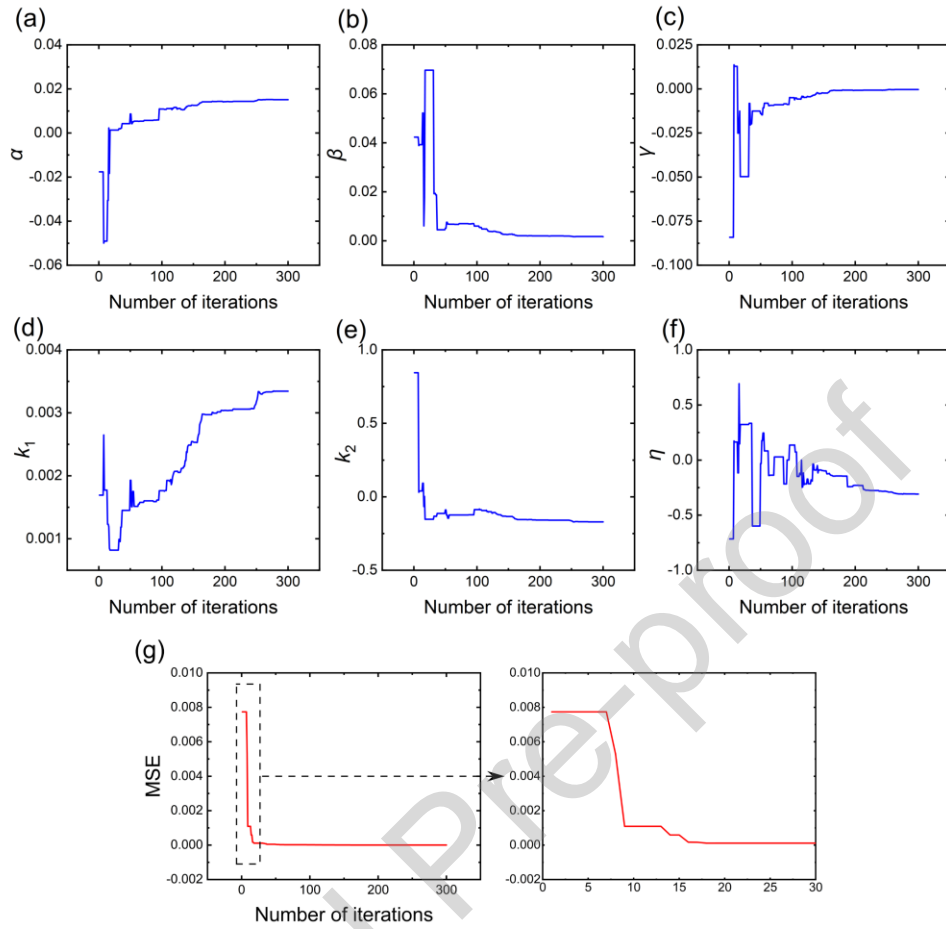


Fig. 7 Iterative processes for the six parameters of the improved Bouc-Wen model (a)-(f) and the mean square error between identified data and experimental data (g).

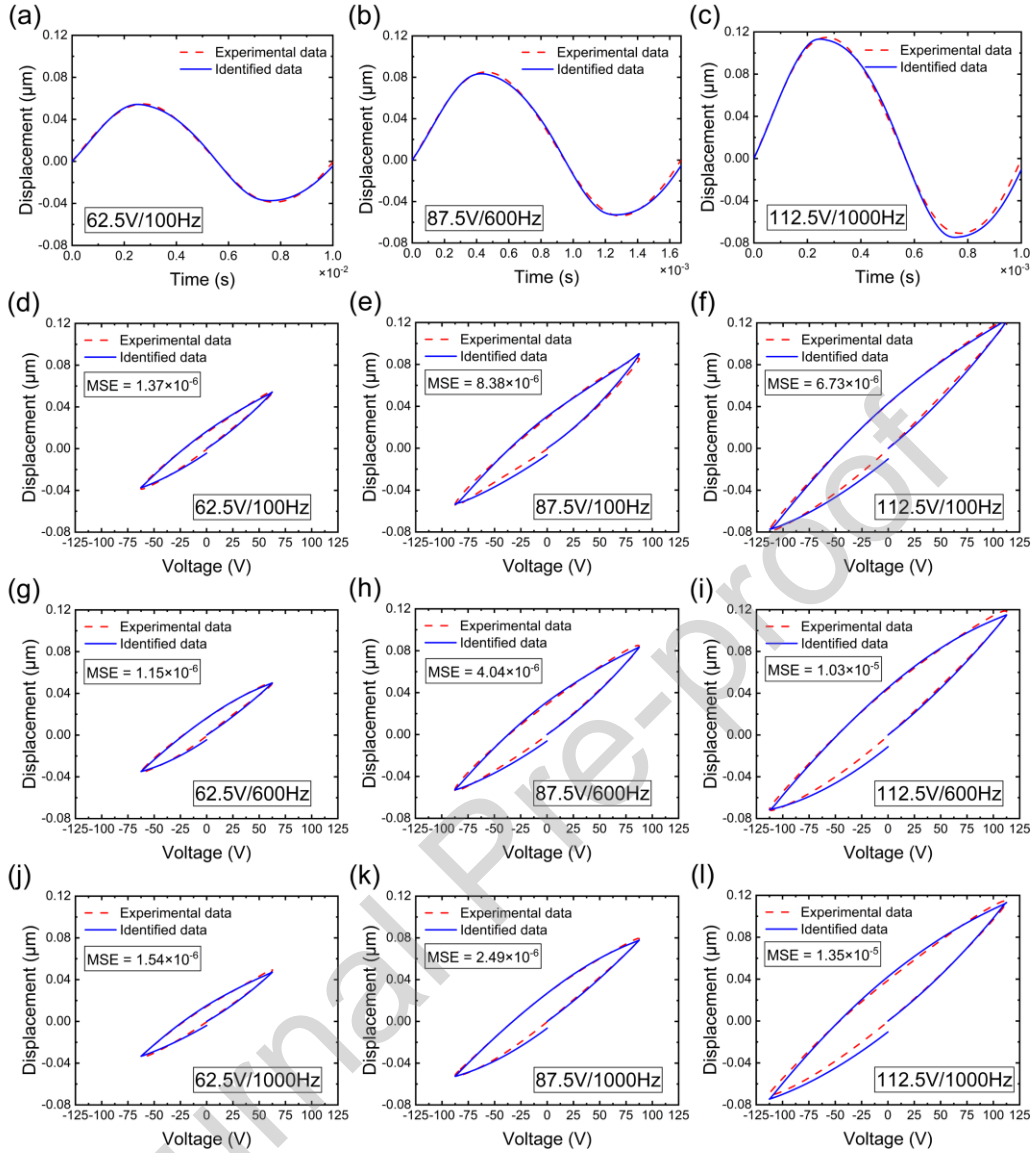


Fig. 8 (a)-(c) Displacement data comparison of identified data and experimental data under different voltages and frequencies, (d)-(l) comparison of hysteresis loop curves under different voltages and frequencies.

At the same voltage and frequency, multiple identifications for each parameter of the Bouc-Wen model were also conducted to eliminate the randomness of the PSO calculation. Then, these six parameters were fitted by the cubic polynomial surfaces with the consideration of both variations of electric field and frequency as shown in Fig. 9. The coefficient values of the polynomial function with the same form as Eq. (11) are listed in Table 4. The purpose of using polynomial fitting was to obtain the concise analytical expression, so that it could be written into the finite element (FE) program. Combined with the piezoelectric constitutive equations already in FE, the following

analysis for the piezoelectric displacement under coupled electrical and mechanical loads can be implemented.

It can be observed that  $\beta$ ,  $\gamma$  and  $k_1$  display an obvious variation with the electric field strength. In particular, the variation of  $\beta$  (in Fig. 9(b)) decreases with the increase of the electric field strength, while  $\gamma$  and  $k_1$  increases with the increase of electric field strength. The other parameters show relatively weak trends. With the change of frequency, the value of each parameter fluctuates very slightly but without obvious trend, which is consistent with the phenomenon found with the experimental data reported in Section 3.1 whereby the characteristic parameters of the hysteresis loop were seen to be affected by the electric field strength more than by the frequency.

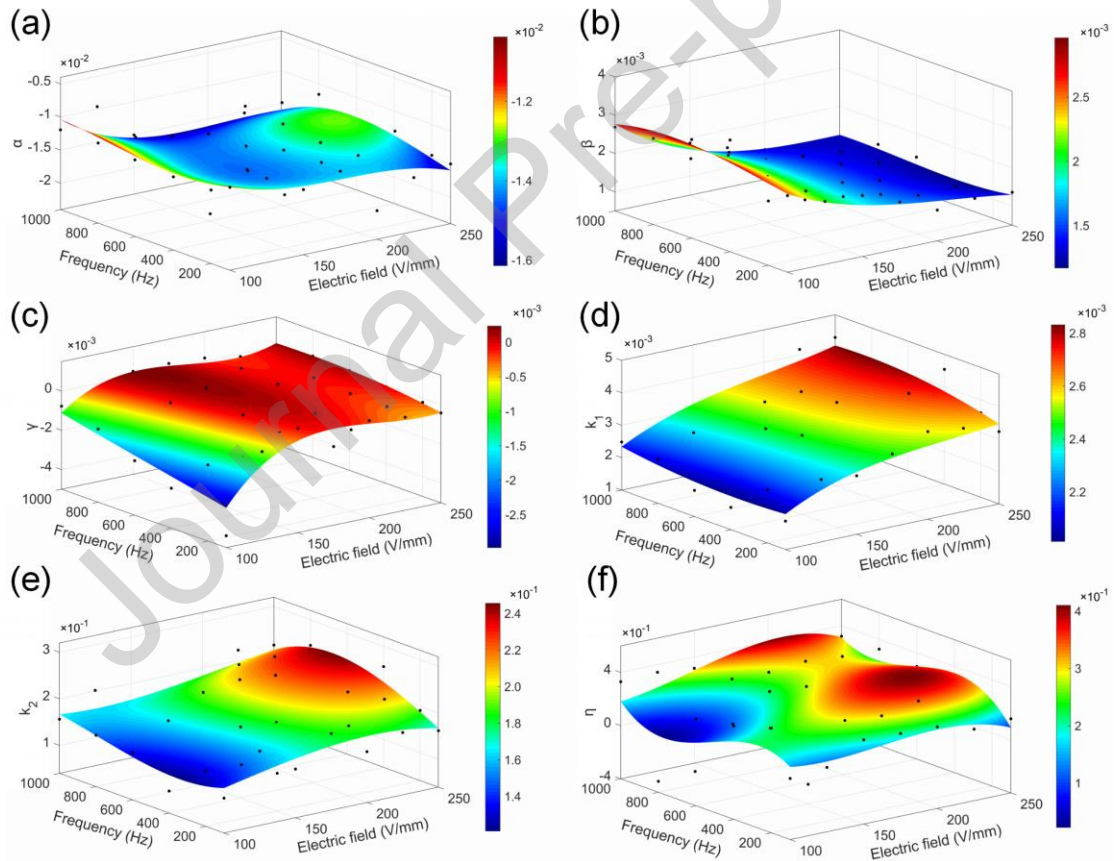


Fig. 9 Variations of the six parameters of the Bouc-Wen model with electric field and frequency.

It can be found that the fitting results of amplitude and width of hysteresis loop, piezoelectric coefficient and hysteresis value versus electric field strength and frequency in Fig. (4)-Fig. (6) all exhibit much clearer dependences than the six

parameters in Fig. 9. This is because that the six parameters in the Bouc-Wen model are the coefficients of the differential equations and have no specific physical meaning. Hence, unlike the characteristic parameters of hysteresis that physically related to the electric field strength and frequency, their variations with the electric field and frequency were just calculated numerically.

Table 4 Coefficient values of the polynomial function of each Bouc-Wen model parameter.

$C_{xx}$	$\alpha(E, f)$	$\beta(E, f)$	$\gamma(E, f)$	$k_1(E, f)$	$k_2(E, f)$	$\eta(E, f)$
$C_{00}$	$1.61 \times 10$	6.11	$-2.55 \times 10$	-2.41	$1.20 \times 10$	$1.01 \times 10^2$
$C_{10}$	$-4.77 \times 10^{-1}$	$-5.97 \times 10^{-2}$	$3.80 \times 10^{-1}$	$7.32 \times 10^{-2}$	$-5.62 \times 10^{-3}$	-2.01
$C_{01}$	$-1.54 \times 10^{-2}$	$3.88 \times 10^{-3}$	$7.13 \times 10^{-3}$	$-1.65 \times 10^{-3}$	$-2.96 \times 10^{-2}$	$7.79 \times 10^{-2}$
$C_{20}$	$2.66 \times 10^{-3}$	$2.76 \times 10^{-4}$	$-1.86 \times 10^{-3}$	$-3.27 \times 10^{-4}$	$6.09 \times 10^{-4}$	$1.26 \times 10^{-2}$
$C_{11}$	$-4.36 \times 10^{-5}$	$-3.66 \times 10^{-5}$	$-6.94 \times 10^{-5}$	$8.44 \times 10^{-6}$	$1.06 \times 10^{-5}$	$1.19 \times 10^{-3}$
$C_{02}$	$4.00 \times 10^{-5}$	$-5.15 \times 10^{-7}$	$4.87 \times 10^{-7}$	$2.03 \times 10^{-6}$	$6.35 \times 10^{-5}$	$-4.14 \times 10^{-4}$
$C_{30}$	$-5.11 \times 10^{-6}$	$-4.50 \times 10^{-7}$	$2.97 \times 10^{-6}$	$5.00 \times 10^{-7}$	$-2.19 \times 10^{-6}$	$-2.57 \times 10^{-5}$
$C_{21}$	$5.37 \times 10^{-7}$	$6.21 \times 10^{-8}$	$1.95 \times 10^{-7}$	$2.26 \times 10^{-8}$	$7.86 \times 10^{-7}$	$-1.17 \times 10^{-6}$
$C_{12}$	$-1.38 \times 10^{-7}$	$1.18 \times 10^{-8}$	$-7.54 \times 10^{-9}$	$-1.26 \times 10^{-8}$	$-2.53 \times 10^{-7}$	$-5.81 \times 10^{-7}$
$C_{03}$	$-1.22 \times 10^{-8}$	$-1.20 \times 10^{-9}$	$2.01 \times 10^{-10}$	$-4.64 \times 10^{-12}$	$-1.62 \times 10^{-8}$	$3.04 \times 10^{-7}$
R-Square	0.2328	0.8812	0.7004	0.7723	0.5171	0.3908

### 3.3 Displacement prediction with the proposed model

The above electric field- and rate-dependent parameters of the Bouc-Wen model were used to predict the piezoelectric ceramic shear motion under different voltage and frequency excitations. Fig. 10 shows eight samples of predicted displacements as compared with the identified parameters, and their error curves based on the experimental data, which are within the conditions listed in Table 1. It can be seen that the curves of the predicted displacement and the measured displacement overlap well with each other at different conditions of voltages and frequencies, and the predicted error mainly occurs at the positions where displacement reaches its maximum value,

which becomes larger under higher excitation signal. In these eight samples given, the maximum error is 7.9 nm. Due to the fact that the piezoelectric coefficient,  $d_{15}$ , and the hysteresis value,  $H_{disp}$ , are calculated by using the geometric parameters of the hysteresis loop,  $A_{Max}$  and  $W_{Max}$ , only the error rates of  $A_{Max}$  and  $W_{Max}$  are analysed as shown in Table 5. It was achieved that the error rates from 0.1% to 12.4% of  $A_{Max}$  and from 1.1% to 14.3% of  $W_{Max}$ , which indicates the effectiveness of the proposed model and the mediocre goodness of fits on the identified parameters of Bouc-Wen model could produce better displacement predictions. This is due to that the shape of a hysteresis loop is determined by these six parameters together, and each parameter is not independent but restricts each other. When keeping other parameters unchanged, the change of  $\alpha$ ,  $\beta$  or  $k_2$  will affect the amplitude and width of the hysteresis loop, while the change of  $\gamma$ , or  $k_1$  will mainly affect the amplitude.  $\eta$  determines the symmetry of the hysteresis loop [41]. Hence, the goodness of fit for a single parameter of the Bouc-Wen model does not directly influence the accuracy of the prediction. Meanwhile, it can be found in Fig. 9 that the variation range of each identified parameter is relatively concentrated and small under the ranges of electric field and frequency, which is fully included by the fitting curved surface. Though their fitting performances of  $\alpha$ ,  $k_2$  and  $\eta$  are not good, i.e. weak regularities over electric field and frequency, the absolute differences between their fitted values and their identified values are not significant, which results in that the prediction of hysteresis loop would not produce significant errors.

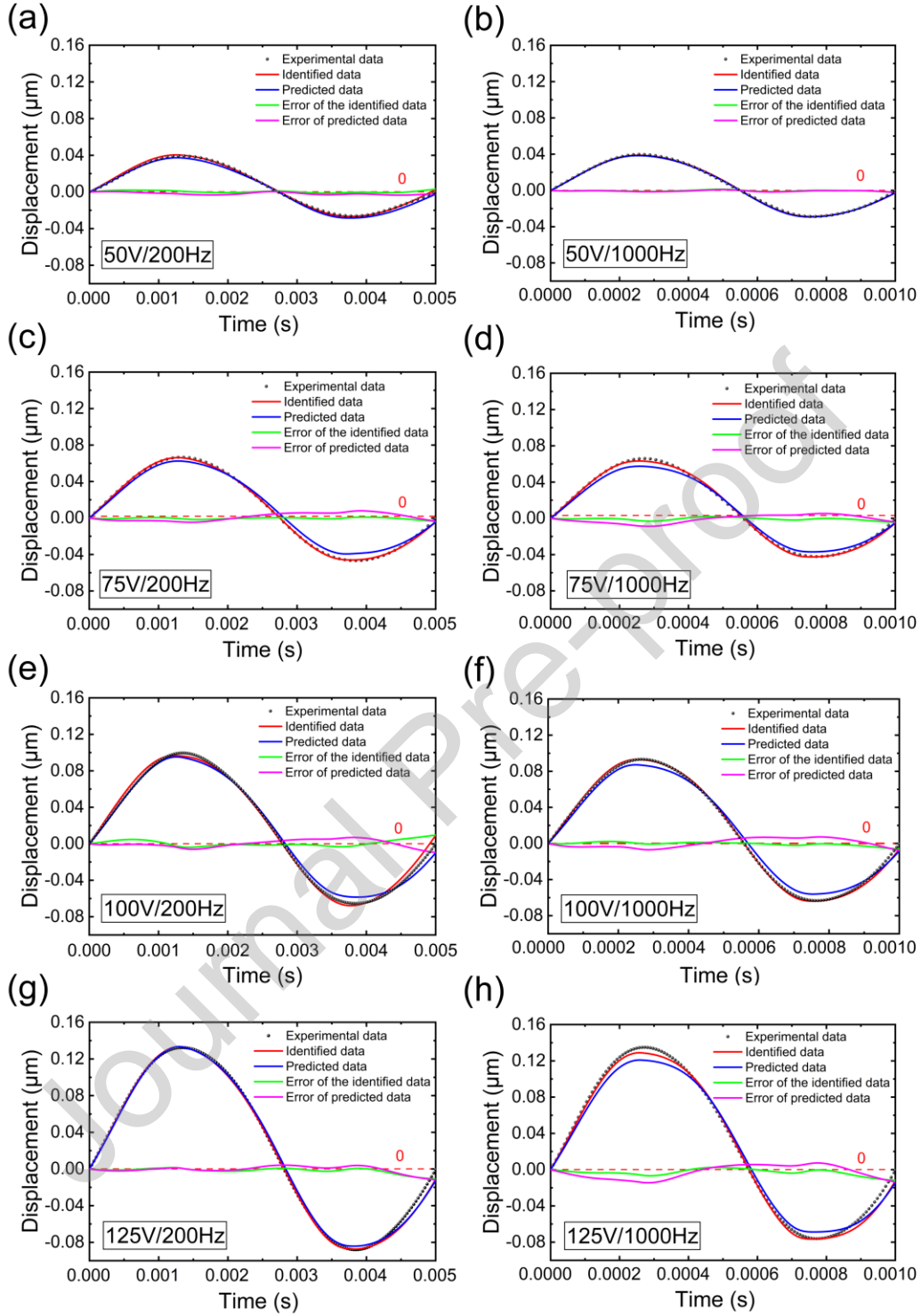


Fig. 10 Comparisons of the predicted displacement, the identified displacement and the experimental displacement.

Table 5 The error rates between the predicted data and the experimental data.

Error rate	$A_{Max}$	$W_{Max}$
50V/200Hz	0.1%	1.1%

50V/1000Hz	1.4%	11.4%
75V/200Hz	9.5%	14.3%
75V/1000Hz	12.4%	6.6%
100V/200Hz	6.8%	5.8%
100V/1000Hz	8.3%	3.1%
125V/200Hz	1.2%	4.5%
125V/1000Hz	10.0%	10.3%

The predicted  $A_{Max}$  and  $W_{Max}$  under conditions of electric field and frequency that were not in the experimental data sample set were verified by comparing with the characteristic parameters of the hysteresis loop calculated by the equations in Table 2, and their error rates were obtained as shown in Fig. 11(a) and (b). The operating condition within or outside the experimental parameter range, i.e. the identification range of the electric field (from 100 V/mm to 250 V/mm) and frequency (from 100 Hz to 1000 Hz), as listed in Table 1 is specified. The blue region (140 V/mm-220 V/mm and 50 Hz-700 Hz) represents the range within the experimental parameter range, but the employed electric field and frequency points do not coincide with those in Table 1. It can be found that in the identification range the maximum error rate of  $A_{Max}$  was less than 16.5% (in the range from 0.1% to 16.5%), and the maximum error rate of width of  $W_{Max}$  is less than 14.5% (in the range from 2.7% to 14.5%). In the pink region, the parameters were chosen outside the identification range (80 V/mm and 260 V/mm, 50 Hz and 1100 Hz), from which it can be seen obviously that much larger error rates were produced. Based on the results in Fig. 11(a) and (b), the distributions of the error rate values under different conditions of electric field and frequency were statistically analysed as shown in Fig. 11(c) and (d). It can be seen that the error rates of more than 15% are almost caused by the conditions that outside the identification range, while within the identification range much smaller error rates (less than 15%) of the prediction can be achieved. Hence, it can be concluded that the prediction effectiveness of the proposed field- and rate-dependent Bouc-Wen model is closely related to the

identification range, and it would not work well when predicting the condition of the electric field and frequency outside the range within which the data points are used to identify the Bouc-Wen model. This may result from the cubic polynomial surface fittings for the variations of the six parameters in Bouc-Wen model in Fig. 9, which would have a poor prediction when the surface extends beyond the identified condition range. Hence, to predict more conditions, larger parameter range is needed first to identify the model parameter.

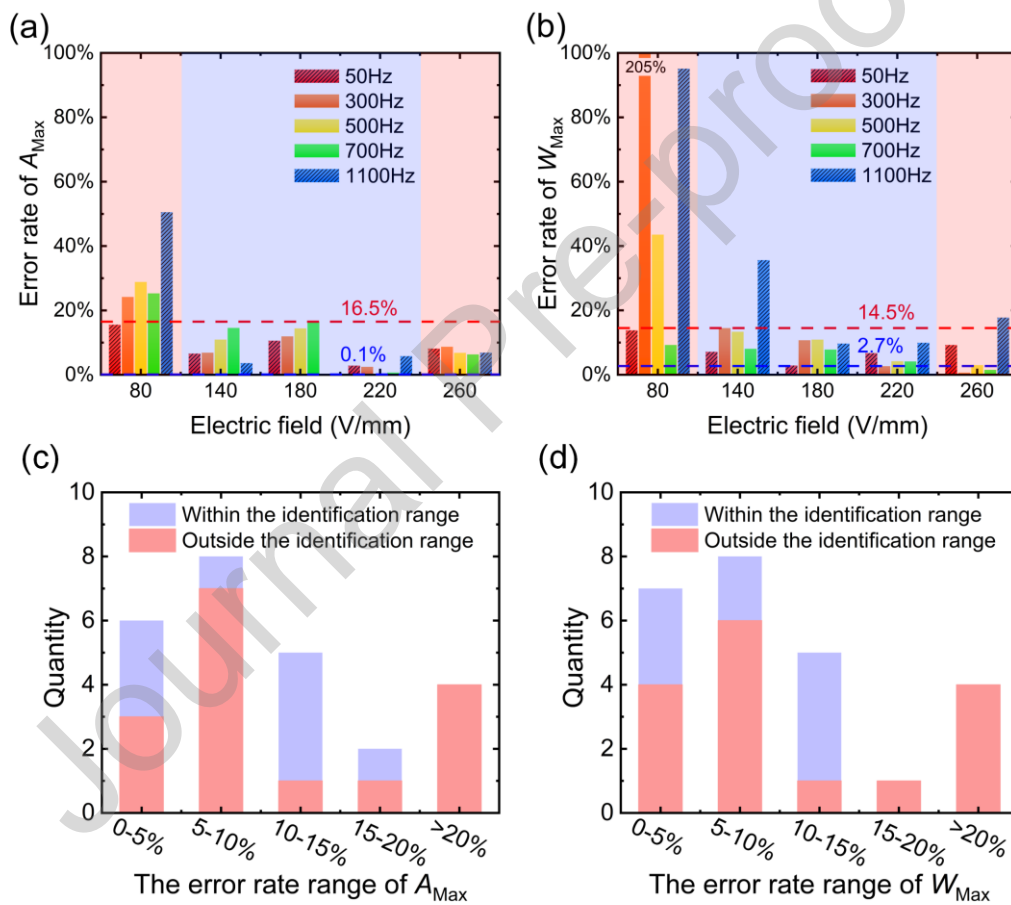


Fig. 11 The error rates of the predicted data of (a) hysteresis loop amplitude and (b) hysteresis loop width under the conditions if not being in the experimental data sample set (Table 1). (c) and (d) are the corresponding statistic distributions of the error rates.

### 3.4 FE analysis with the proposed model

After achieving a satisfactory description of hysteresis properties, the obtained mathematical model can be employed to correct the hysteresis nonlinearity of the

piezoelectric actuator by the inverse compensation of the input voltage, the effectiveness of which has been extensively verified in the fields of precision positioning and sensing [18, 24, 41]. In addition, the direct and converse piezoelectric effects under different conditions are usually analysed through the FE modelling, which is based on the electromechanical constitutive equations of the piezoelectric material [49-52]. In these equations, the relationship between the electrical and mechanical quantities is linked by the piezoelectric coefficients, which is electric field- and rate-dependent as analysed above. However, most studies use constant piezoelectric coefficients in FE-based simulation models. In our previous work [53], a FE model with the dependent  $d_{15}(E, f)$  was developed. While the FE simulation presented in this previous report could accurately predict the movement displacement, it cannot accurately describe the movement trajectory, as the  $d_{15}(E, f)$  is calculated from the displacement amplitude under each condition of the electric field ( $E$ ) and frequency ( $f$ ). As compared to the discrete data distribution of the experimental data, the identified electric field- and rate-dependent Bouc-Wen model with the reasonable effectiveness and able to be described by the mathematical expressions is more applicable for the analysis of piezoelectric displacement under coupled field loads. Hence, an enhanced FE modelling method is presented here to investigate the electrical and mechanical coupled effect on the hysteresis nonlinearity.

Fig. 12 shows the flow chart of the FE modelling approach. A shear plate meshed by the piezoelectric element (C3D8E) and applied boundary conditions (e.g. fixed mode, mechanical load and electrical load) was created in Abaqus/CAE. The inp file of the model was then generated, which initially had a constant  $d_{15}$ . According to the electrical condition  $E(f)$ , the hysteresis loop was calculated based on the electric field- and rate-dependent Bouc-Wen model in MATLAB. Following that, a time-varying  $d_{15}(t)$  of one hysteresis loop can be obtained by calculating each point of the curve with Eq. (9). Due to the feature of the hysteresis loop, at the positions where  $E$  equals 0, the displacement does not return to the initial position, which causes  $d_{15}$  to approach infinity and mislead the displacement prediction. In data processing, such values of  $d_{15}$  are removed, which would result in an incomplete hysteresis loop

obtained but with little impact on the analysis. Then,  $d_{15}(t)$  at  $E(f)$  is written into the generated inp file to replace the constant  $d_{15}$  via the calling of a Python code. Combining with user subroutine USDFLD to capture the electric field- and rate-dependence, the modified inp field is submitted to Abaqus/Standard solver to simulate the motion of the shear piezoelectric plate under coupled field loads.

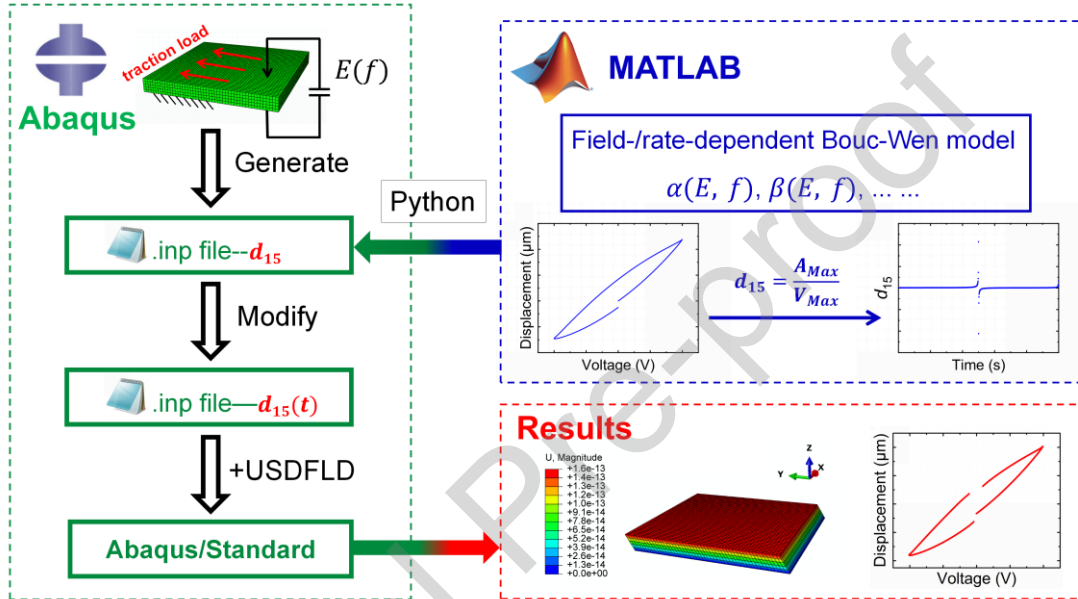


Fig. 12 Implementation flowchart of the coupled mechanical-electrical FE analysis by using the proposed electric field- and rate-dependent Bouc-Wen model.

A sinusoidal electrical excitation of  $E=200$  V/mm and  $f=200$  Hz and four type of mechanical traction loads all with the amplitude of 10 N as shown in Fig. 13(a1)-(a4) were applied to the plate, and the simulated results are shown in Fig. 13(b1)-(b4). By comparing with Fig. 10(c), it can be seen under the condition of 0 N in (b1) that the FE reproduces the displacement predicted by the proposed model, which has a reasonable agreement with the experimental displacement. In fact, the comparison between the FE model and the experimental data is the same as the comparison between the proposed model and the experimental data, as the FE model employs the  $d_{15}$  calculated by the proposed model and also combines with the piezoelectric constitutive equations. Hence, with the hysteresis behaviour taken into account, both the displacement amplitude and the movement trajectory can be well described by the developed FE model. From the simulation results, it can also be found that a force will

produce a proportional displacement offset along the force direction. The offset would increase, or decrease, the output displacement of the actuator, if it is in the same, or opposite, direction, respectively. Fig. 14 shows the effect of load type on the hysteresis loop. The change in displacement causes the loop to shift and rotate. The opening widths ( $W_{Max}$ ) under these four types of loads are almost identical, which depends on the difference in force values between the two zero points of the driving voltage. There are obvious differences in amplitude ( $A_{Max}$ ) between them. This is caused by the difference in force at the amplitude of driving voltage.

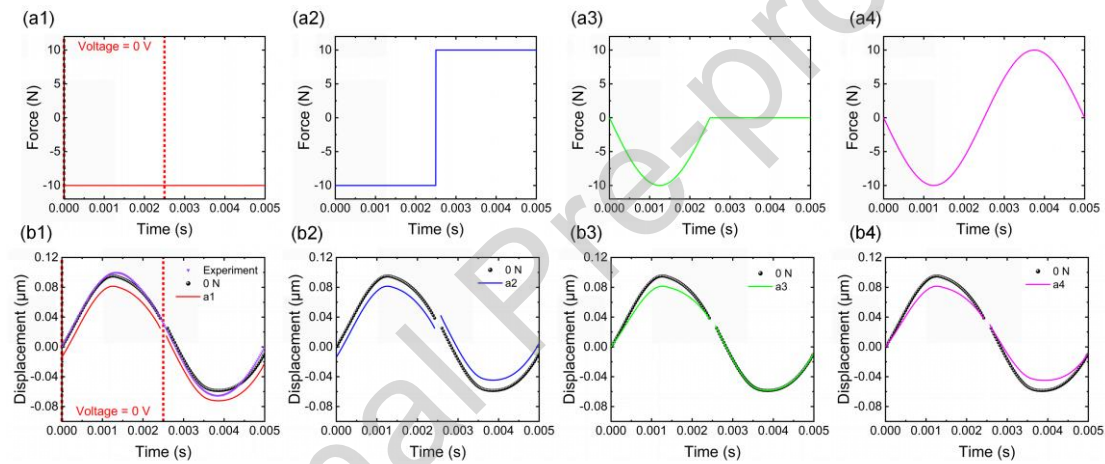


Fig. 13 Motion simulation of the piezoelectric ceramics shear plate under coupled field loads. (a1)-(a4) Simulated boundary conditions for the mechanical load, (b1)-(b4) corresponding simulated outcomes of the piezoelectric displacements.

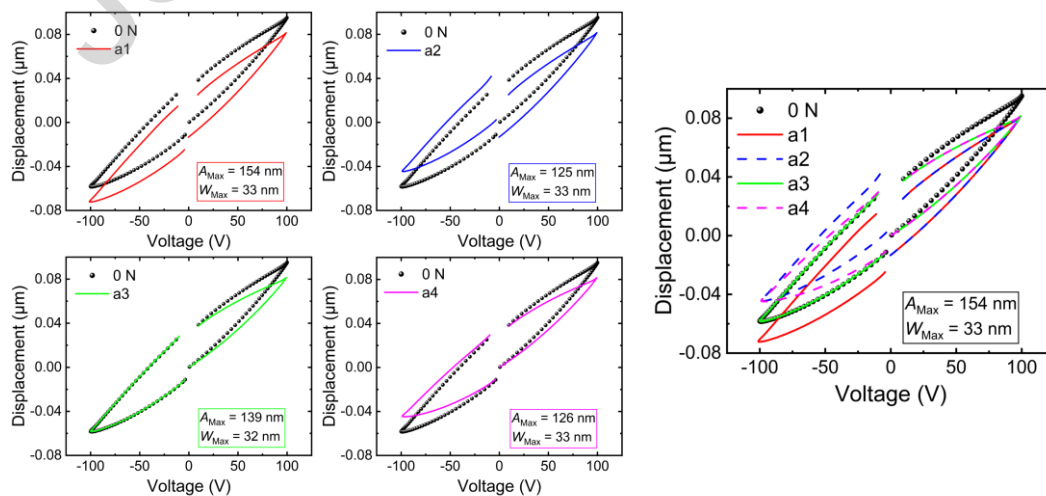


Fig. 14 Simulation analysis for the effect of load type on the hysteresis loop.

Fig. 15 shows another four types of time-varying mechanical loads. Fig. 15(a) is applied a force with the trapezoidal wave variation and Fig. 15(b) is with the semi-sinusoidal variation. It can be found from these two conditions that when the difference in force values around the two zero points of the driving voltage is not zero, the opening width of the hysteresis loop will change according to the size of the difference. Fig. 15(c) and (d) are under two sinusoidal forces but with opposite directions. It can be seen that if the force around the zero points of the driving voltage is opposite to the moving direction, the opening width can be reduced, while the force in the same direction of motion will increase the opening width.

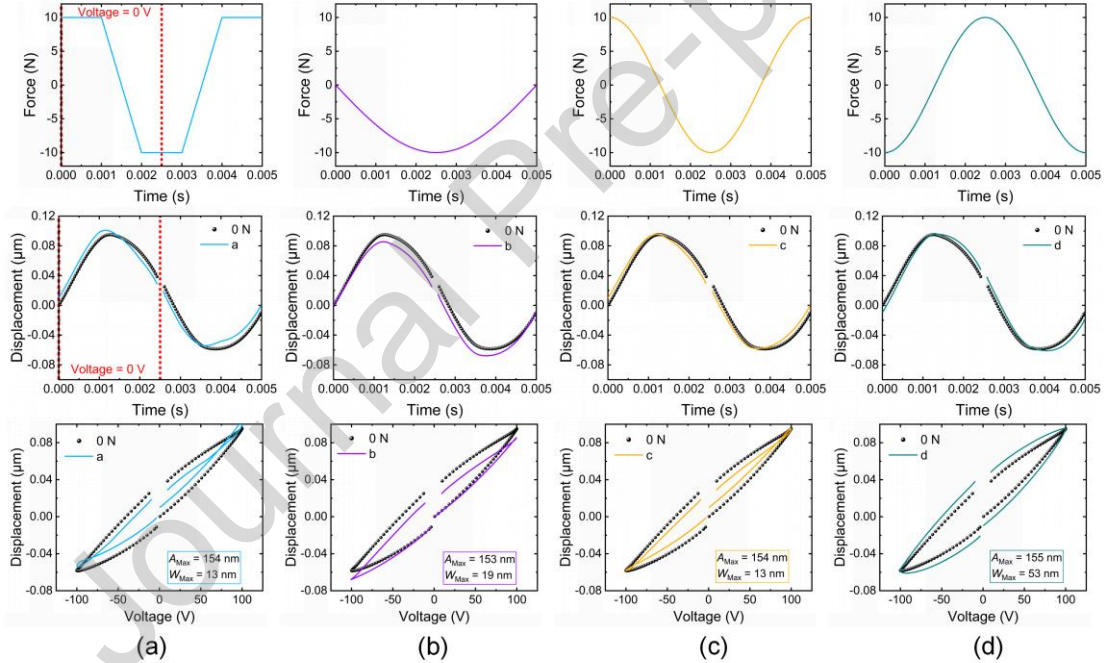


Fig. 15 Motion simulation of the piezoelectric ceramics shear plate under coupled field loads.

#### 4. Conclusions

To accurately characterise the hysteresis nonlinearity of the shear motion of piezoelectric ceramic under high voltage and high frequency excitations, an electric field- and rate-dependent Bouc-Wen model was implemented, and the effectiveness of its prediction was validated by analysing the effect of the electric field strength and frequency on hysteresis. Characteristic parameters, namely amplitude, width,

piezoelectric coefficient and hysteresis value, of hysteresis loops were used to describe the hysteretic nonlinearity of a shear-type piezoelectric stack. The Bouc-Wen model was identified under different voltages and frequencies using the PSO algorithm. With the characterization of field- and rate-dependent parameters in the Bouc-Wen model, the displacement of the shear motion of piezoelectric ceramics was then predicted, and a good agreement with experimental data was found. The derived electric field- and rate-dependent Bouc-Wen model was also combined with the FE method, and the FE simulation of the movement with hysteresis property of a piezoelectric actuator was achieved. In particular, with the proposed FE modelling, the dynamic behaviour of the actuator under different electrical and mechanical coupled field loads could be analysed.

The analysis of the electric field- and rate-dependent hysteresis revealed that the piezoelectric coefficient increases with the electric field strength and decreases when the frequency increases, which determines the displacement of the shear motion. The hysteresis value becomes larger as the electric field strength increases, while it is less affected by the frequency. The prediction results of the proposed model show that the error rates of the hysteresis loop amplitude and width are respectively less than 16.5%, and 14.5% in the identified range of electric field and frequency.

## **Acknowledgements**

The authors gratefully acknowledge the financial supports from the National Natural Science Foundation of China (52105434), the China Postdoctoral Science Foundation (2022M710642) and the Talent Introduction Program of Northeast Forestry University (520/60201487).

## **References**

[1] Z. Liu, H. Wu, W. Ren, Z.G. Ye, Piezoelectric and ferroelectric materials: Fundamentals, recent progress, and applications, third ed. 2023. <https://doi.org/10.1016/B978-0-12-823144-9.00069-8>.

- [2] S.T. Ho, S.J. Jan, A piezoelectric motor for precision positioning applications, *Precis. Eng.* 43 (2016) 285-293. <https://doi.org/10.1016/j.precisioneng.2015.08.007>.
- [3] J.H. Park, M.Y. Seo, Y.B. Ham, S.N. Yun, D.I. Kim, A study on high-output piezoelectric micropumps for application in DMFC, *J. Electroceram.* 30 (2013) 102-107. <https://doi.org/10.1007/s10832-012-9740-5>.
- [4] H.K. Ma, R.H. Chen, Y.H. Hsu, Development of a piezoelectric-driven miniature pump for biomedical applications, *Sensor. Actuat. A-Phys.* 234 (2015) 23-33. <https://doi.org/10.1016/j.sna.2015.08.003>.
- [5] M. Li, J.X. Yuan, D. Guan, W. Chen, Application of piezoelectric fiber composite actuator to aircraft wing for aerodynamic performance improvement, *Sci. China Technol. Sc.* 54 (2011) 395-402. <https://doi.org/10.1007/s11431-010-4212-0>.
- [6] X. Zhang, Y. Tan, A hybrid model for rate-dependent hysteresis in piezoelectric actuators, *Sensor. Actuat. A-Phys.* 157 (2010) 54-60. <https://doi.org/10.1016/j.sna.2009.10.009>.
- [7] D.A. Hall, Review nonlinearity in piezoelectric ceramics, *J. Mater. Sci.* 36 (2001) 4575-4601. <https://doi.org/10.1023/A:1017959111402>.
- [8] P.J. Chen, S.T. Montgomery, A macroscopic theory for the existence of the hysteresis and butterfly loops in ferroelectricity, *Ferroelectrics*, 23 (1) (1980) 199-207. <https://doi.org/10.1080/00150198008018803>.
- [9] R.B. Mrad, H. Hu, A model for voltage-to-displacement dynamics in piezoceramic actuators subject to dynamic-voltage excitations, *IEEE-ASME T. Mech.* 7 (4) (2002) 479-489. <https://doi.org/10.1109/TMECH.2002.802724>.
- [10] J. Gan, X. Zhang, A review of nonlinear hysteresis modeling and control of piezoelectric actuators, *AIP Adv.* 9 (4) (2019). <https://doi.org/10.1063/1.5093000>.
- [11] V. Hassani, T. Tjahjowidodo, T.N. Do, A survey on hysteresis modeling, identification and control, *Mech. Syst. Signal Pr.* 49 (1-2) (2014) 209-233. <https://doi.org/10.1016/j.ymssp.2014.04.012>.
- [12] C. Ru, L. Chen, B. Shao, W. Rong, L. Sun, A hysteresis compensation method of piezoelectric actuator: Model, identification and control, *Control Eng. Pract.* 17 (9) (2009) 1107-1114. <https://doi.org/10.1016/j.conengprac.2009.04.013>.

- [13] G.Y. Gu, M.J. Yang, L.M. Zhu, Real-time inverse hysteresis compensation of piezoelectric actuators with a modified Prandtl-Ishlinskii model, *Rev. Sci. Instrum.* 83 (6) (2012). <https://doi.org/10.1063/1.4728575>.
- [14] M. Al Janaideh, M. Al Saaideh, M. Rakotondrabe, On hysteresis modeling of a piezoelectric precise positioning system under variable temperature, *Mech. Syst. Signal Pr.* 145 (2020), 106880. <https://doi.org/10.1016/j.ymssp.2020.106880>.
- [15] F. Ikhouane, V. Mañosa, J. Rodellar, Dynamic properties of the hysteretic Bouc-Wen model, *Syst. Control Lett.* 56 (3) (2007) 197-205. <https://doi.org/10.1016/j.sysconle.2006.09.001>.
- [16] W. Zhu, D. Wang, Non-symmetrical Bouc-Wen model for piezoelectric ceramic actuators, *Sensor. Actuat. A-Phys.* 181 (2012) 51-60. <https://doi.org/10.1016/j.sna.2012.03.048>.
- [17] G. Wang, G. Chen, F. Bai, Modeling and identification of asymmetric Bouc–Wen hysteresis for piezoelectric actuator via a novel differential evolution algorithm, *Sensor. Actuat. A-Phys.* 235 (2015) 105-118. <https://doi.org/10.1016/j.sna.2015.09.043>.
- [18] M. Rakotondrabe, Bouc–Wen modeling and inverse multiplicative structure to compensate hysteresis nonlinearity in piezoelectric actuators, *IEEE T. Autom. Sci. Eng.* 8(2) (2010) 428-431. <https://doi.org/10.1109/TASE.2010.2081979>.
- [19] M. Al Janaideh, M. Rakotondrabe, I. Al-Darabsah, O. Aljanaideh, Internal model-based feedback control design for inversion-free feedforward rate-dependent hysteresis compensation of piezoelectric cantilever actuator, *Control Eng. Pract.* 72 (2018) 29-41. <https://doi.org/10.1016/j.conengprac.2017.11.001>.
- [20] Y.D. Tao, H.X. Li, L.M. Zhu, Rate-dependent hysteresis modeling and compensation of piezoelectric actuators using Gaussian process, *Sensor. Actuat. A-Phys.* 295 (2019) 357-365. <https://doi.org/10.1016/j.sna.2019.05.046>.
- [21] M.J. Yang, C.X. Li, G.Y. Gu, L.M. Zhu, Modeling and compensating the dynamic hysteresis of piezoelectric actuators via a modified rate-dependent Prandtl–Ishlinskii model, *Smart Mater. Struct.* 24 (12) (2015), 125006. <https://doi.org/10.1088/0964-1726/24/12/125006>.
- [22] Y. Xu, X. Li, X. Yang, Z. Yang, L. Wu, A two-stage model for rate-dependent inverse

hysteresis in reluctance actuators, *Mech. Syst. Signal Pr.* 135 (2020), 106427. <https://doi.org/10.1016/j.ymssp.2019.106427>.

[23] J. Gan, X. Zhang, An enhanced Bouc-Wen model for characterizing rate-dependent hysteresis of piezoelectric actuators, *Rev. Sci. Instrum.* 89 (11) (2018). <https://doi.org/10.1063/1.5038591>.

[24] S. Kang, H. Wu, Y. Li, X. Yang, J. Yao, A fractional-order normalized Bouc–Wen model for piezoelectric hysteresis nonlinearity, *IEEE-ASME T. Mech.* 27 (1) (2021) 126-136. <https://doi.org/10.1109/TMECH.2021.3058851>.

[25] A.G. Muthalif, M.K.M. Razali, N.H.D. Nordin, S.B.A. Hamid, Parametric estimation from empirical data using particle swarm optimization method for different magnetorheological damper models, *IEEE Access*, 9 (2021) 72602-72613. <https://doi.org/10.1109/ACCESS.2021.3080432>.

[26] A. Benjeddou, Shear-mode piezoceramic advanced materials and structures: a state of the art, *Mech. Adv. Mater. Struc.* 14 (4) (2007) 263-275. <https://doi.org/10.1080/15376490600809336>.

[27] J. Wang, Y. Yan, Z. Li, Y. Geng, Towards understanding the machining mechanism of the atomic force microscopy tip-based nanomilling process, *Int. J. Mach. Tool Manu.* 162 (2021), 103701. <https://doi.org/10.1016/j.ijmachtools.2021.103701>.

[28] S. Chang, Y. Geng, Y. Yan, Tip-Based Nanomachining on Thin Films: A Mini Review, *Nanomanuf Metrol.* 5 (2022) 2–22. <https://doi.org/10.1007/s41871-021-00115-5>.

[29] J.L. Ha, R.F. Fung, C.S. Yang, Hysteresis identification and dynamic responses of the impact drive mechanism, *J. Sound Vib.* 283 (3-5) (2005) 943-956. <https://doi.org/10.1016/j.jsv.2004.05.032>.

[30] M. Ismail, F. Ikhouane, J. Rodellar, The hysteresis Bouc-Wen model, a survey, *Arch. Comput. Method. E.* 16 (200) 161-188. <https://doi.org/10.1007/s11831-009-9031-8>.

[31] H. Qin, N. Bu, W. Chen, Z. Yin, An asymmetric hysteresis model and parameter identification method for piezoelectric actuator, *Math. Probl. Eng.* 2014 (2014). <https://doi.org/10.1155/2014/932974>.

- [32] M. Ye, X. Wang, Parameter estimation of the Bouc–Wen hysteresis model using particle swarm optimization, *Smart Mater. Struct.* 16 (6) (2007), 2341. <https://doi.org/10.1088/0964-1726/16/6/038>.
- [33] D. Wang, D. Tan, L. Liu, Particle swarm optimization algorithm: an overview, *Soft Comput.* 22 (2018) 387-408. <https://doi.org/10.1007/s00500-016-2474-6>.
- [34] R. Eberhart, J. Kennedy, A new optimizer using particle swarm theory, MHS'95. Proceedings of the Sixth International Symposium on Micro Machine and Human Science, Nagoya, 1995, pp. 39-43. <https://doi.org/10.1109/MHS.1995.494215>.
- [35] Y. Shi, R. Eberhart, A modified particle swarm optimizer, in: 1998 IEEE International Conference on Evolutionary Computation Proceedings. IEEE World Congress on Computational Intelligence (Cat. No.98TH8360), Anchorage, 1998, pp. 69-73. <https://doi.org/10.1109/ICEC.1998.699146>.
- [36] S.U. Khan, S. Yang, L. Wang, L. Liu, A modified particle swarm optimization algorithm for global optimizations of inverse problems, *IEEE T. Magn.* 52 (3) (2015) 1-4. <https://doi.org/10.1109/TMAG.2015.2487678>.
- [37] M. Clerc, J. Kennedy, The particle swarm-explosion, stability, and convergence in a multidimensional complex space, *IEEE T. Evolut. Comput.* 6 (1) (2002) 58-73. <https://doi.org/10.1109/4235.985692>.
- [38] Q.M. Zhang, W.Y. Pan, L.E. Cross, Laser interferometer for the study of piezoelectric and electrostrictive strains, *J. Appl. Phys.* 63 (8) (1988) 2492-2496. <https://doi.org/10.1063/1.341027>.
- [39] H. Zhan, W. Zhou, L. Ran, H. Yu, B. Peng, R. Hao, A high-resolution optical displacement detection method for piezoelectric microvibratory stage, *IEEE T. Ind. Electron.* 67 (12) (2020) 10897-10904. <https://doi.org/10.1109/TIE.2019.2962414>.
- [40] F. Ikhouane, J.E. Hurtado, J. Rodellar, Variation of the hysteresis loop with the Bouc–Wen model parameters, *Nonlinear Dynam.* 48 (2007) 361-380. <https://doi.org/10.1007/s11071-006-9091-3>.
- [41] Q. Zhang, Y. Dong, Y. Peng, J. Luo, S. Xie, H. Pu, Asymmetric Bouc–Wen hysteresis modeling and inverse compensation for piezoelectric actuator via a genetic algorithm–based particle swarm optimization identification algorithm, *J. Intel. Mat. Syst.*

- Str. 30 (8) (2019) 1263-1275. <https://doi.org/10.1177/1045389X19831360>.
- [42] O. Aljanaideh, S. Rakheja, C.Y. Su, Experimental characterization and modeling of rate-dependent asymmetric hysteresis of magnetostrictive actuators, *Smart Mater. Struct.* 23 (3) (2014), 035002. <https://doi.org/10.1088/0964-1726/23/3/035002>.
- [43] S. Li, W. Cao, L.E. Cross, The extrinsic nature of nonlinear behavior observed in lead zirconate titanate ferroelectric ceramic, *J. Appl. Phys.* 69 (10) (1991) 7219-7224. <https://doi.org/10.1063/1.347616>.
- [44] J.E. Garcia, R. Perez, D.A. Ochoa, A. Albareda, M.H. Lente, J.A. Eiras, Evaluation of domain wall motion in lead zirconate titanate ceramics by nonlinear response measurements, *J. Appl. Phys.* 103 (5) (2008). <https://doi.org/10.1063/1.2894595>.
- [45] M. Otonicar, M. Dragomir, T. Rojac, Dynamics of domain walls in ferroelectrics and relaxors, *J. Am. Ceram. Soc.* 105 (11) (2022) 6479-6507. <https://doi.org/10.1111/jace.18623>.
- [46] V. Kannan, D.M. Kochmann, Rate-dependent ferroelectric switching in barium titanate ceramics from modified PUND experiments, *Extreme Mech. Lett.* 57 (2022), 101898. <https://doi.org/10.1016/j.eml.2022.101898>.
- [47] P. Li, F. Yan, C. Ge, X. Wang, L. Xu, J. Guo, P. Li, A simple fuzzy system for modelling of both rate-independent and rate-dependent hysteresis in piezoelectric actuators, *Mech. Syst. Signal Pr.* 36 (1) (2013) 182-192. <https://doi.org/10.1016/j.ymssp.2012.10.004>.
- [48] M. Al Janaideh, S. Rakheja, C.Y. Su, Experimental characterization and modeling of rate-dependent hysteresis of a piezoceramic actuator, *Mechatronics*, 19 (5) (2009) 656-670. <https://doi.org/10.1016/j.mechatronics.2009.02.008>.
- [49] L. Qin, J. Jia, M. Choi, K. Uchino, Improvement of electromechanical coupling coefficient in shear-mode of piezoelectric ceramics, *Ceram. Int.* 45 (2) (2019) 1496-1502. <https://doi.org/10.1016/j.ceramint.2018.10.018>.
- [50] Y. Kuang, M. Zhu, Evaluation and validation of equivalent properties of macro fibre composites for piezoelectric transducer modelling, *Compos. Part B-Eng.* 158 (2019) 189-197. <https://doi.org/10.1016/j.compositesb.2018.09.068>.
- [51] P.C. Ramegowda, D. Ishihara, R. Takata, T. Niho, T. Horie, Finite element analysis

of a thin piezoelectric bimorph with a metal shim using solid direct-piezoelectric and shell inverse-piezoelectric coupling with pseudo direct-piezoelectric evaluation, *Compos. Struct.* 245 (2020), 112284. <https://doi.org/10.1016/j.compstruct.2020.112284>.

[52] N. Lv, C Zhong, L. Wang, Bending vibration characteristics of the piezoelectric composite double laminated vibrator, *Ceram. Int.* 47 (22) (2021) 31259-31267. <https://doi.org/10.1016/j.ceramint.2021.07.302>.

[53] B. Xue, E. Brousseau, C. Bowen, Modelling of a shear-type piezoelectric actuator for AFM-based vibration-assisted nanomachining, *Int. J. Mech. Sci.* 243 (2023), 108048. <https://doi.org/10.1016/j.ijmecsci.2022.108048>.

#### Biographies



**Ruonan Yin** received a B.S. degree in vehicle engineering from Yantai University in 2021. He is currently a M.S. degree candidate at the College of Mechanical and Electrical Engineering, Northeast Forestry University, Harbin, China. His current research interest lies in the characterization of the nonlinearity of piezoelectric shear-type actuator.



**Bo Xue** received the Ph.D. degree from Harbin Institute of Technology, Harbin, China, in 2018. He is currently an associate Professor at the College of Mechanical and Electrical Engineering, Northeast Forestry University, Harbin, China. His research interest lies in micro-nano machining and measurement with a specific focus on piezoelectric-driven tip-based mechanical machining.



**Emmanuel Brousseau** is a Professor at Cardiff School of Engineering, Cardiff University, Cardiff, United Kingdom. His current research interest lies in the field of advanced manufacturing technologies with a specific focus on nano mechanical machining (i.e. AFM probe-based) and micro thermal machining (i.e laser-based).



**Yanquan Geng** received the Ph.D. degree from Harbin Institute of Technology, Harbin, China, in 2016. He is currently a Professor at the School of Mechanical Engineering, Harbin Institute of Technology, Harbin, China. His research interest lies in micro-nano machining, measurement and application based on AFM.



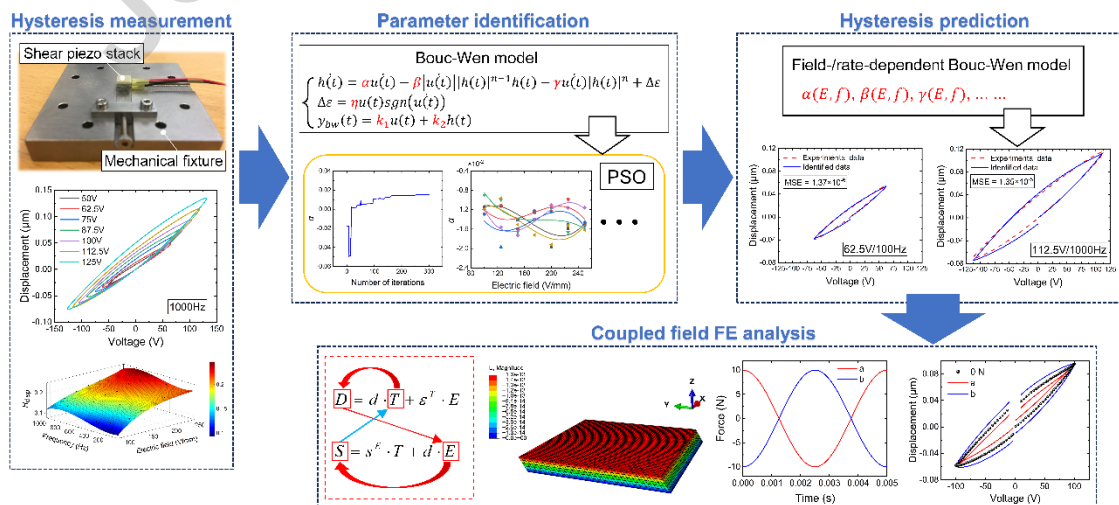
**Yongda Yan** received the Ph.D. degree from Harbin Institute of Technology, Harbin, China, in 2007. He is currently a Professor at the School of Mechanical Engineering, Harbin Institute of Technology, Harbin, China. His research interest lies in micro-nano machining, measurement and application based on AFM.

### Declaration of interests

The authors declare that they have no known competing financial interests or personal relationships that could have appeared to influence the work reported in this paper.

The authors declare the following financial interests/personal relationships which may be considered as potential competing interests:

### Graphical abstract



## Highlights:

- The dependence of hysteresis properties of the piezoelectric shear motion on the electric field and frequency is characterised.
- The Bouc-Wen model is identified by using the PSO algorithm under different conditions of electric fields and frequencies.
- An electric field- and rate-dependent hysteresis model based on the Bouc-Wen model is established.
- A novel FE modelling approach is proposed to analyse the piezoelectric movement under the electrical and mechanical coupled loads.